The New Superconductors

Z. Fisk   UC Irvine

China/US Winter School

Hong Kong   2013

Supported by AFOSR MURI

What does the record tell us?

- What drives materials discovery?
- What is role of theory?
- What constitutes a breakthrough?
- Will there be a room temperature superconductor?

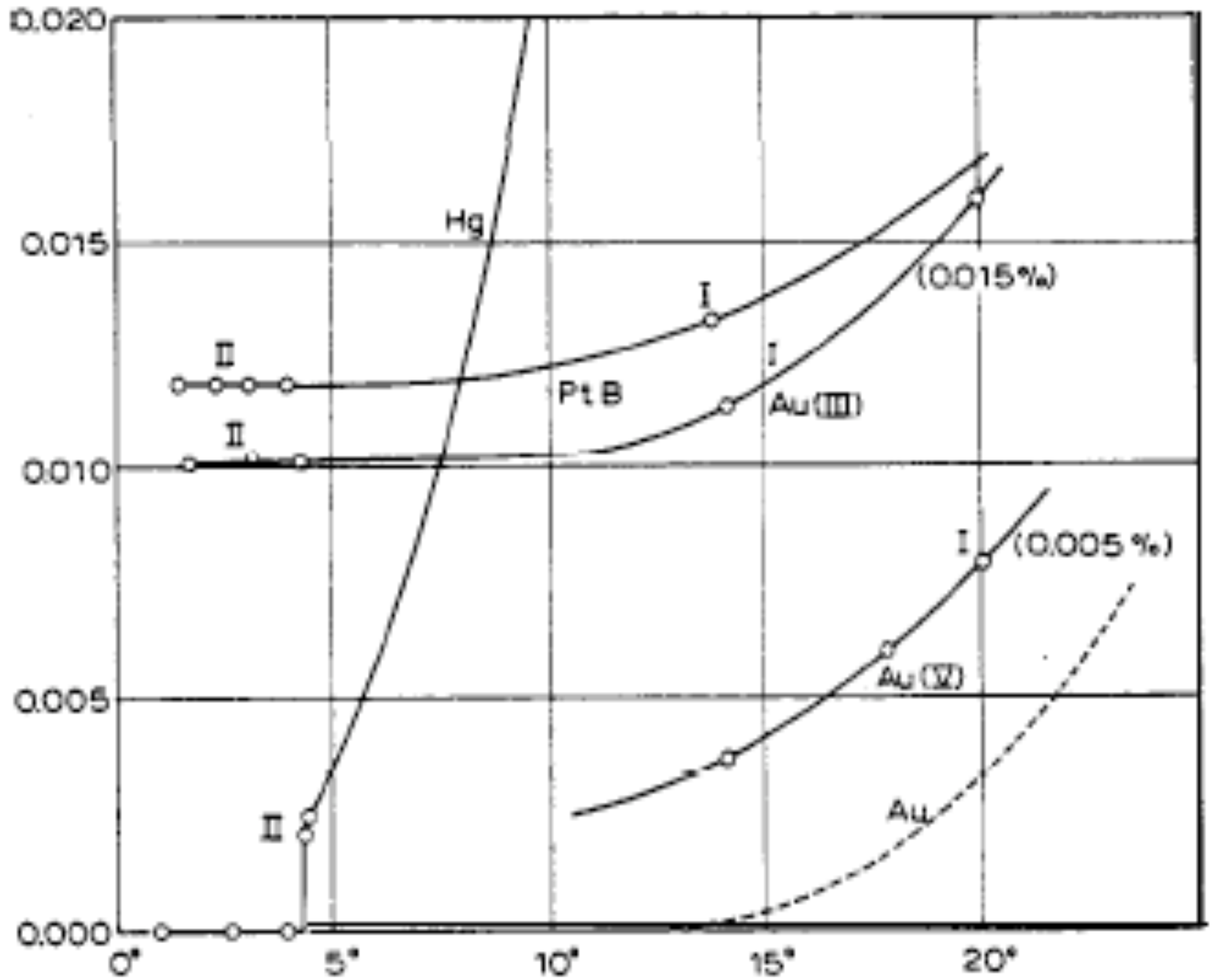

0.020
0.015
0.010
0.005
0.000
0°
5°
10°
15°
20°
Hg
I
II
Pt B
(0.015%)
I
Au (III)
II
I
(0.005%)
Au (V)
II
Au

ambient pressure superconductor: T_c(K), T_c^{max}(K), P(GPa)

high pressure superconductor: T_c^{max}(K), P(GPa)

H																	He
Li 0.0004 14 30	Be 0.026											B 11 250	C	N	O 0.6 100	F	Ne
Na	Mg											Al 1.14	Si 8.2 15.2	P 13 30	S 17.3 190	Cl	Ar
K	Ca 25 161	Sc 19.6 106	Ti 0.39 3.35 56.0	V 5.38 16.5 120	Cr	Mn	Fe 2.1 21	Co	Ni	Cu	Zn 0.875	Ga 1.091 7 1.4	Ge 5.35 11.5	As 2.4 32	Se 8 150	Br 1.4 100	Kr
Rb	Sr 7 50	Y 19.5 115	Zr 0.546 11 30	Nb 9.50 9.9 10	Mo 0.92	Tc 7.77	Ru 0.51	Rh .00033	Pd	Ag	Cd 0.56	In 3.404	Sn 3.722 5.3 11.3	Sb 3.9 25	Te 7.5 35	I 1.2 25	Xe
Cs 1.3 12	Ba 5 18	insert La-Lu	Hf 0.12 8.6 62	Ta 4.483 4.5 43	W 0.012	Re 1.4	Os 0.655	Ir 0.14	Pt	Au	Hg-α 4.153	Tl 2.39	Pb 7.193	Bi 8.5 9.1	Po	At	Rn
Fr	Ra	insert Ac-Lr	Rf	Ha													

La-fcc 6.00 13 15	Ce 1.7 5	Pr	Nd	Pm	Sm	Eu 2.75 142	Gd	Tb	Dy	Ho	Er	Tm	Yb	Lu 12.4 174
Ac	Th 1.368	Pa 1.4	U 0.8(β) 2.4(α) 1.2	Np	Pu	Am 0.79 2.2 6	Cm	Bk	Cf	Es	Fm	Md	No	Lr

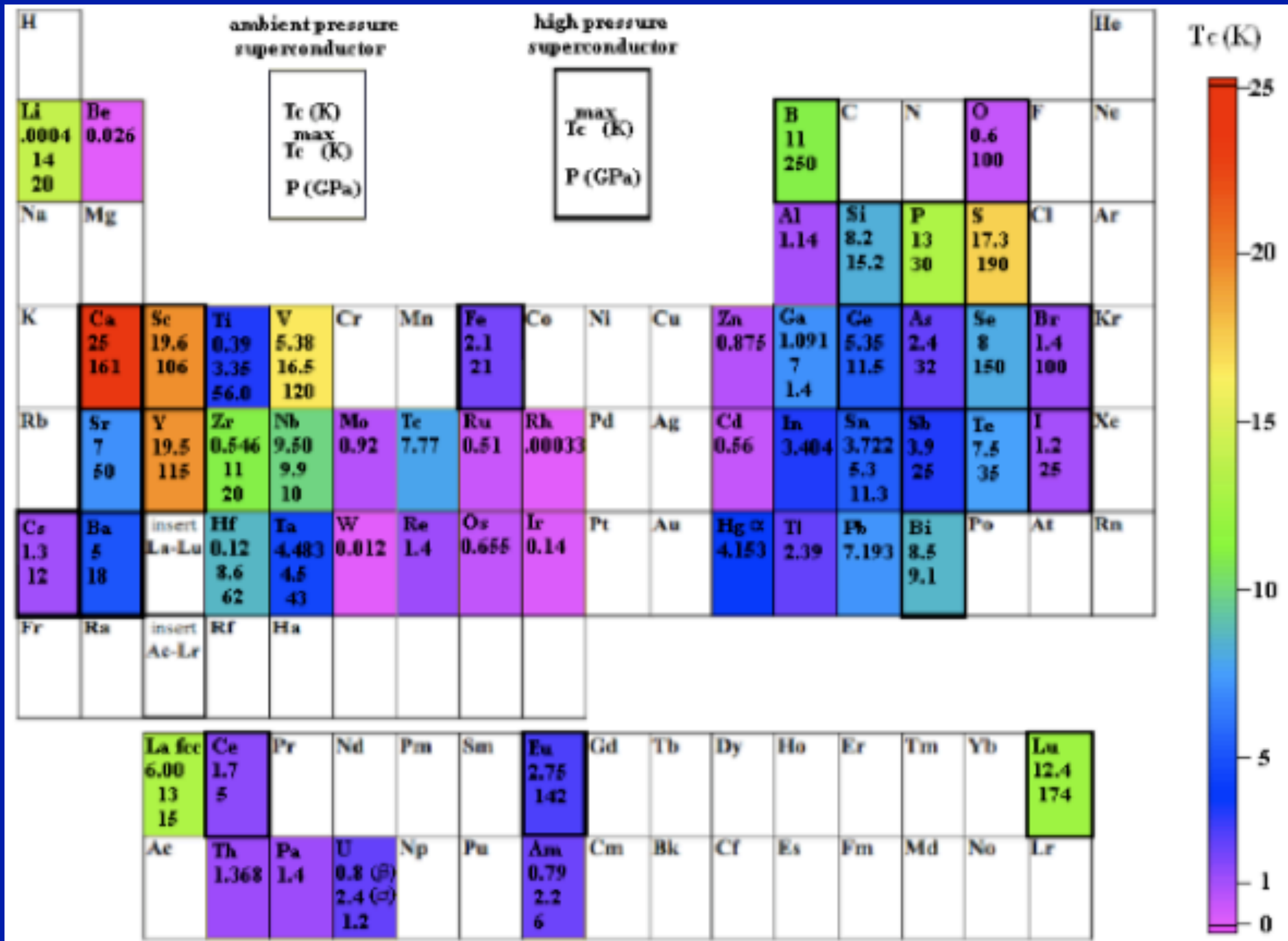
ambient pressure superconductor
Tc (K)
max Tc (K)
P (GPa)
high pressure superconductor
max Tc (K)
P (GPa)
Tc (K)
25
20
15
10
5
1
0
H
He
Li .0004 14 20
Be 0.026
B 11 250
C
N
O 0.6 100
F
Ne
Na
Mg
Al 1.14
Si 8.2 15.2
P 13 30
S 17.3 190
Cl
Ar
K
Ca 25 161
Sc 19.6 106
Ti 0.39 3.35 56.0
V 5.38 16.5 120
Cr
Mn
Fe 2.1 21
Co
Ni
Cu
Zn 0.875
Ga 1.091 7 1.4
Ge 5.35 11.5
As 2.4 32
Se 8 150
Br 1.4 100
Kr
Rb
Sr 7 50
Y 19.5 115
Zr 0.546 11 20
Nb 9.50 9.9 10
Mo 0.92
Tc 7.77
Ru 0.51
Rh .00033
Pd
Ag
Cd 0.56
In 3.404
Sn 3.722 5.3 11.3
Sb 3.9 25
Te 7.5 35
I 1.2 25
Xe
Cs 1.3 12
Ba 5 18
insert La-Lu
Hf 0.12 8.6 62
Ta 4.483 4.5 43
W 0.012
Re 1.4
Os 0.655
Ir 0.14
Pt
Au
Hg α 4.153
Tl 2.39
Pb 7.193
Bi 8.5 9.1
Po
At
Rn
Fr
Ra
insert Ac-Lr
Rf
Ha
La fcc 6.00 13 15
Ce 1.7 5
Pr
Nd
Pm
Sm
Eu 2.75 142
Gd
Tb
Dy
Ho
Er
Tm
Yb
Lu 12.4 174
Ac
Th 1.368
Pa 1.4
U 0.8 (β) 2.4 (α) 1.2
Np
Pu
Am 0.79 2.2 6
Cm
Bk
Cf
Es
Fm
Md
No
Lr

Where do we find superconductivity?

- High temperature phases
- Mo and W films
- Magnetic elements: Fe, Cr
- 4f elements: Ce, Eu
- 5f elements: U, Am
- Cluster compounds

Fig. 1

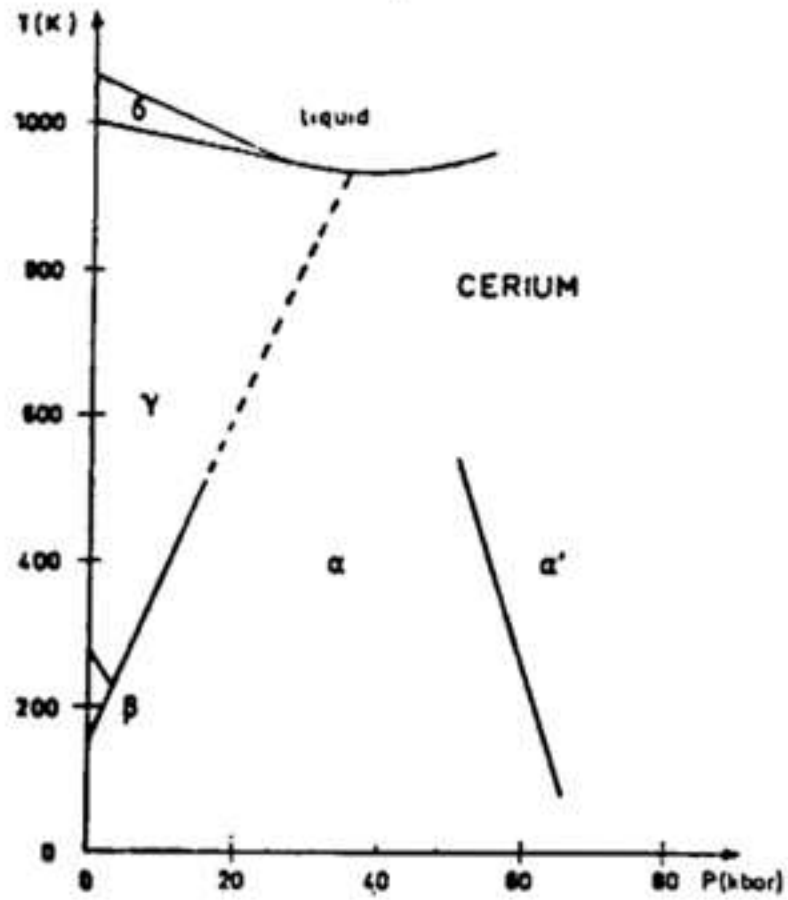

The phase diagram of cerium (δ = b.c.c., γ = f.c.c., β = *dhcp*, α = f.c.c. and α' = f.c.c. or distorted *dhcp*). The extension of the true α–γ transition line meets the minimum point of the melting curve.

Uranium under pressure

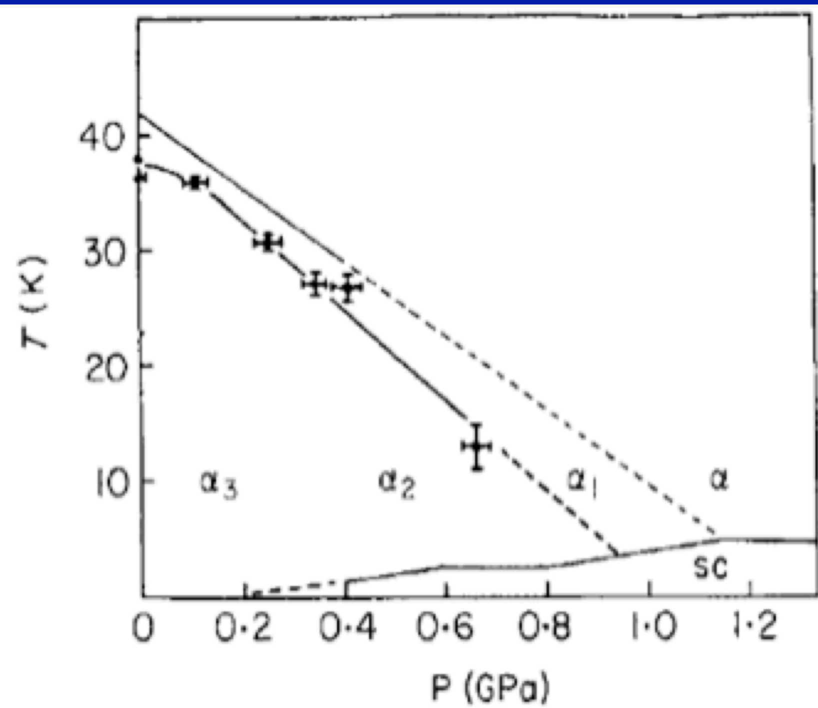

Figure 3 2. The suppression of the 37 K transition, observed by a calorimetric technique, taken from Chu and Knapp (1973). The results are compared to the schematic phase diagram that emerges partly from the results in figure 3.1. The three low-temperature phases are labelled α_1, α_2, and α_3

1950s: the Edisonian approach to discovering new superconductors
and the era of conventional superconductivity

Enrico Fermi

Enrico Fermi (1901–1954)

Fermi: systematics of materials may give a clue

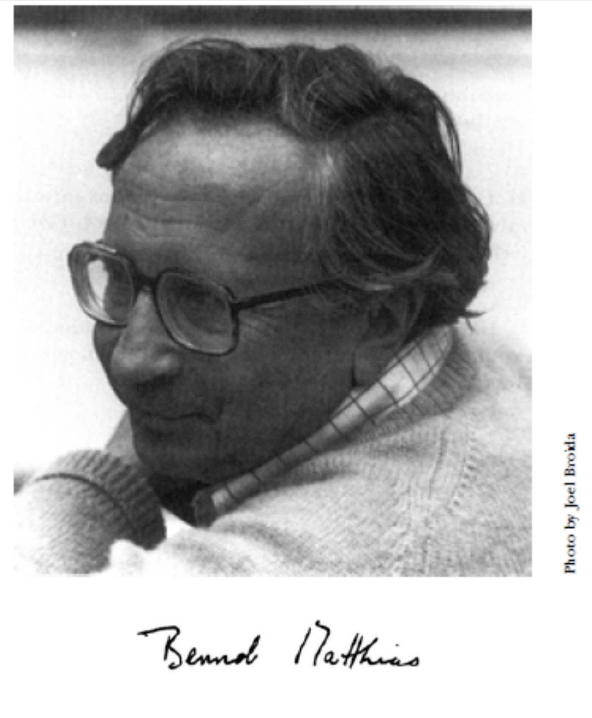

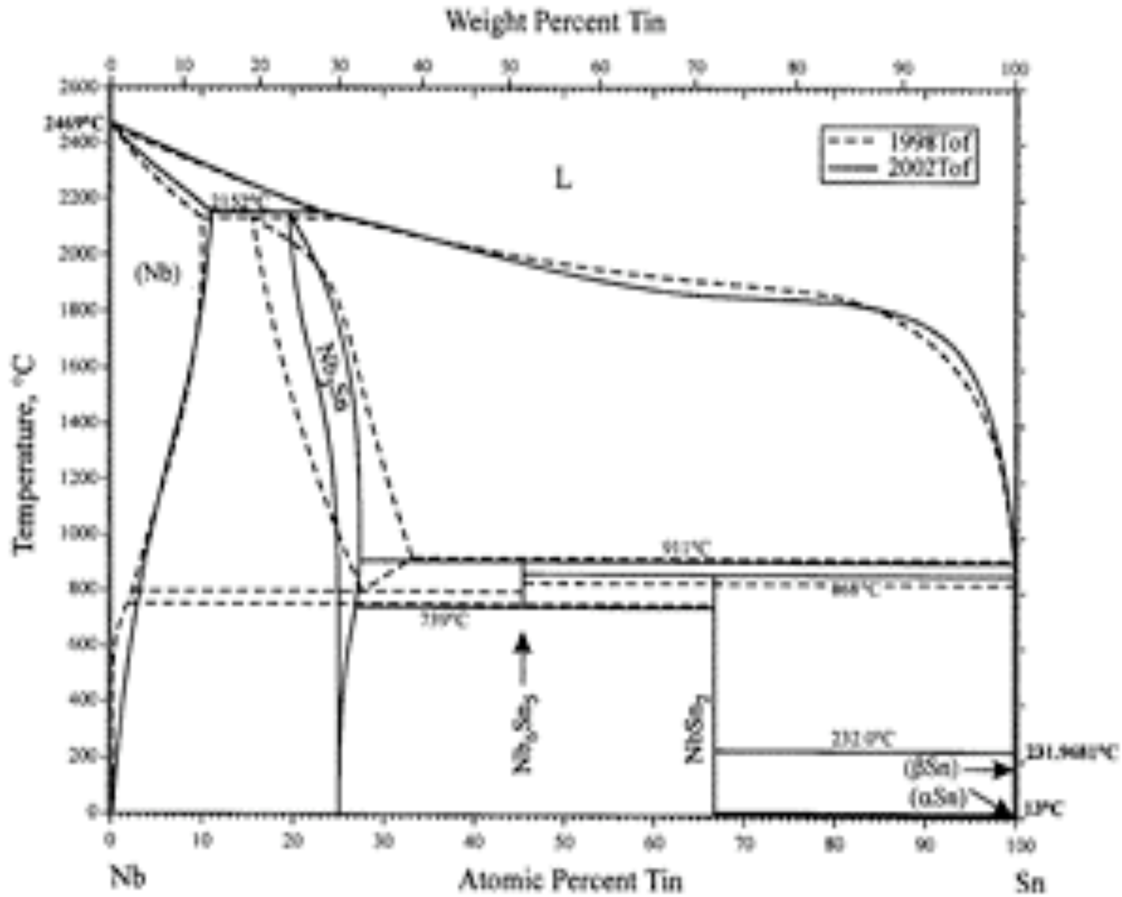

Nb-Sn phase diagram

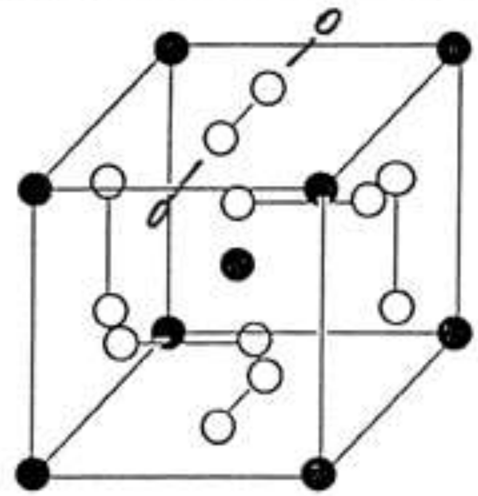

FIGURE 9–7. The V_6Si_2 cubic building block for V_3Si and related A-15 supercor
Shaded circles in the center and at each of the eight vertices correspond to silicc
whereas the pairs of open circles (each linked by a straight line) in each of the :
correspond to vanadium atoms.

reference cube (Figure 9–7), namely one in each face. The V–V bonc vanadium chains, although equivalent in the overall structure, arc following two types relative to a V_6Si_2 reference cube with which ı associated:

1. The first type (A) consists of bonds between two vanadium atc given face of the V_6Si_2 reference cube. Such V–V bonds are sha between the two cubes sharing the face containing the vanadiurr
2. The second type (B) consists of bonds between a vanadium atorr adjacent vanadium atom in the chain *not* associated with th reference cube. Such V–V bonds are shared between four adjace cubes.

Batterman and Barrett   Phys. Rev. **145**, 296 (1966)

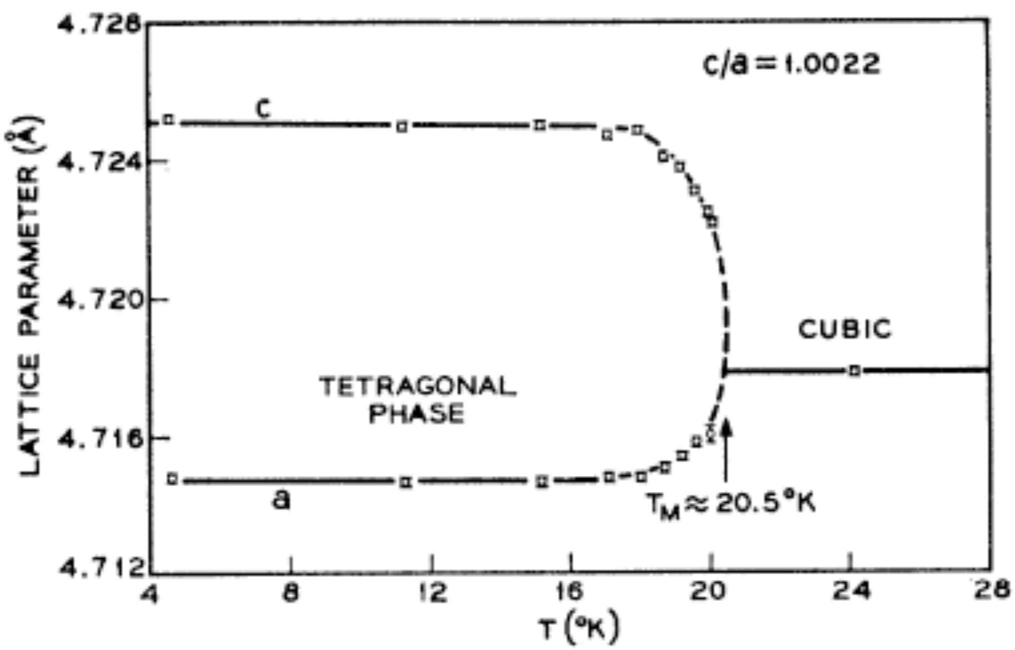

FIG. 6. *c* and *a* parameter versus *T* of a well-behaved specimen. The data in the dashed region were difficult to obtain because of peak overlap and broadening. All evidence indicates that the change is smooth but rapid in this region.

C. W. Chu V_3Si: $T_{Martensitic}$ / T_c

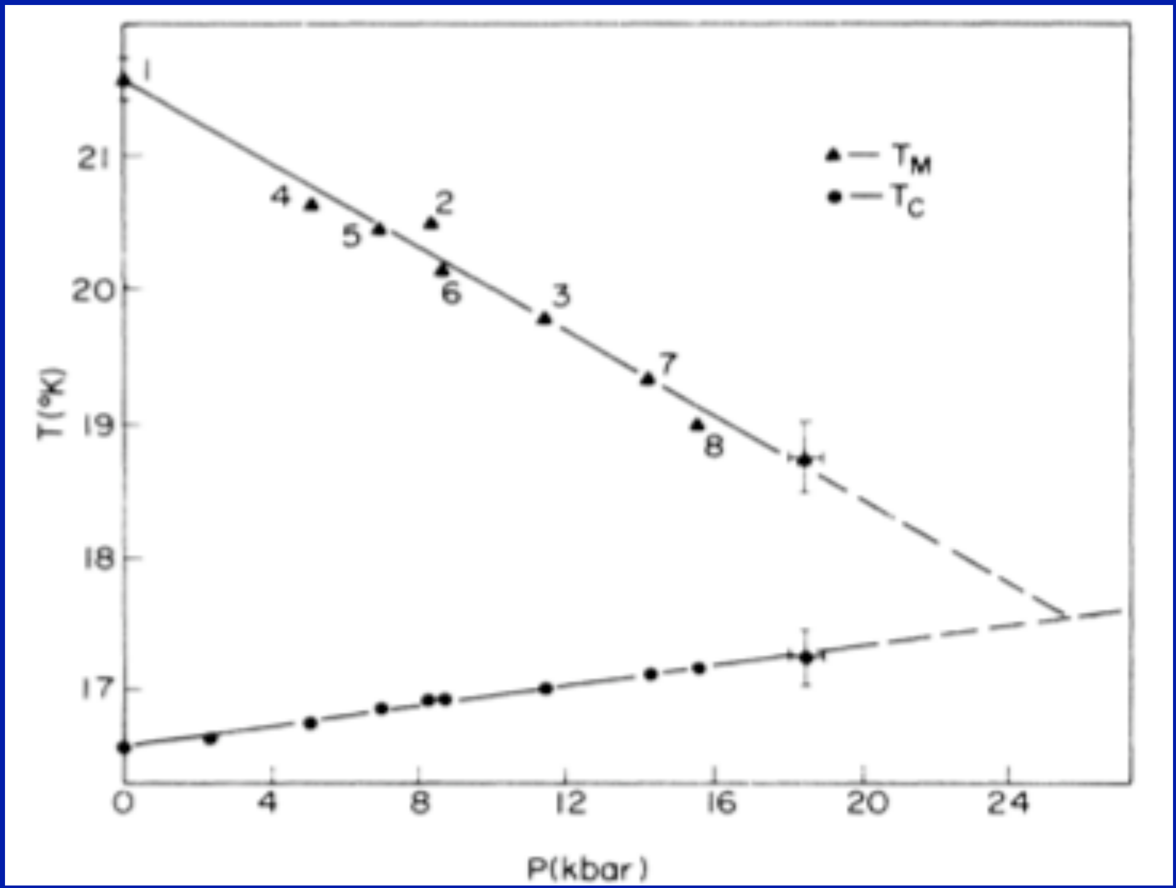

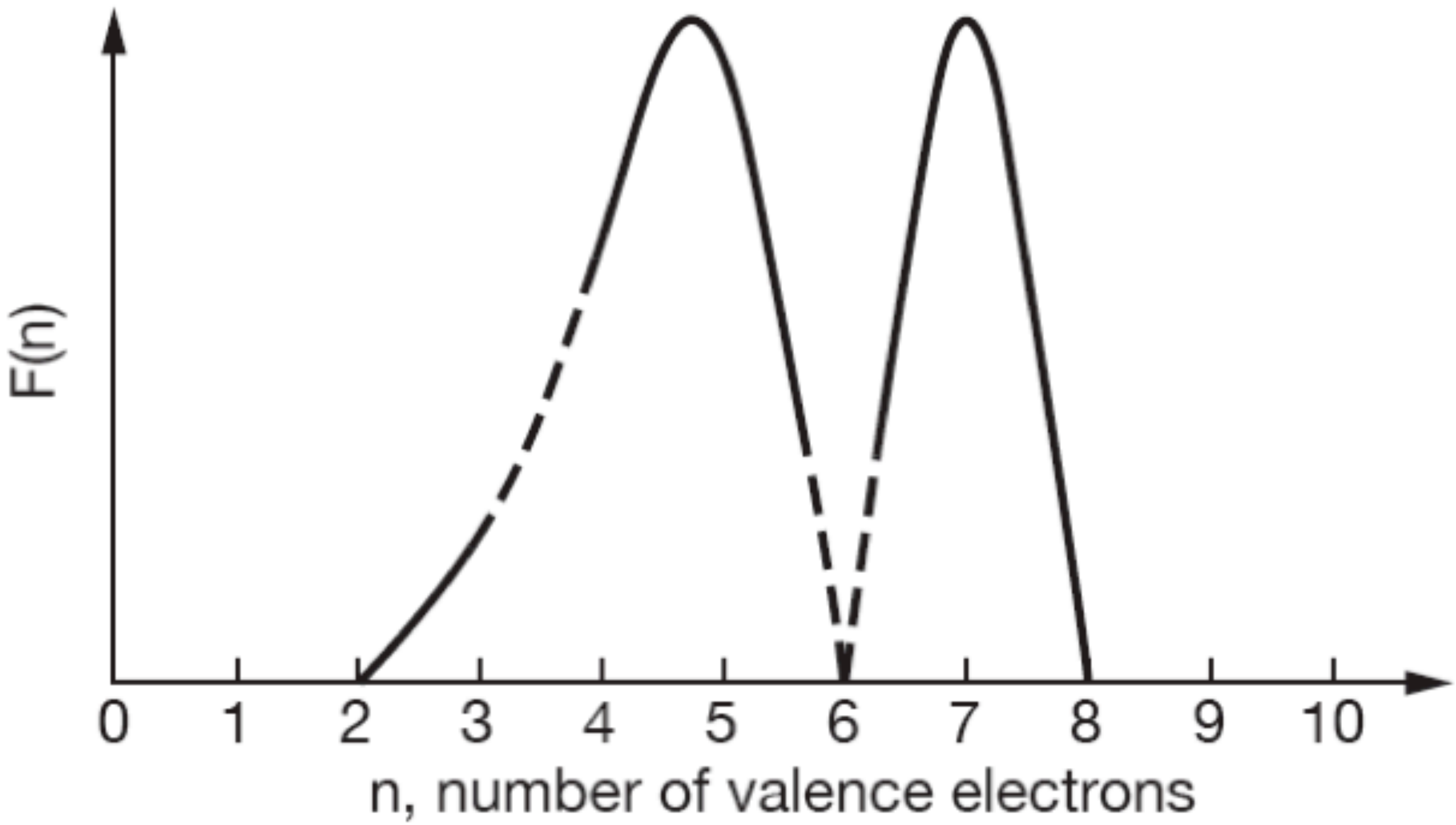

Fig. 3: Trend for superconducting transition temperatures $T_c \sim F(n)$ for superconductivity of elements and binary compounds (from ref. 18)

1957 the Bardeen-Cooper-Schrieffer theory arrives

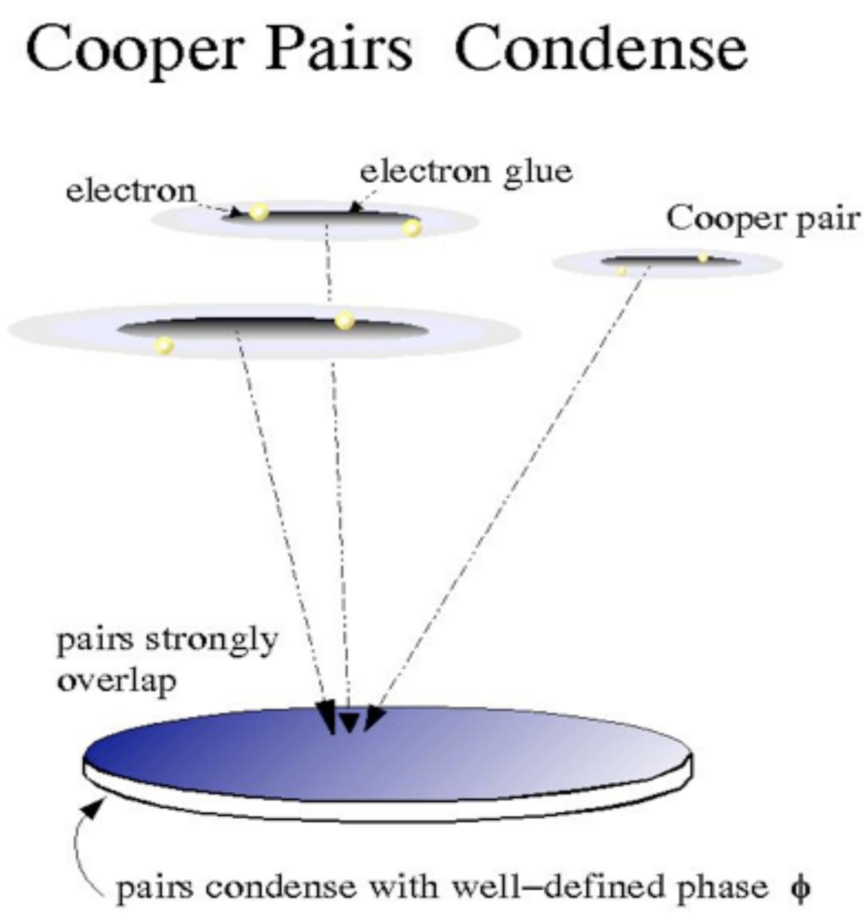

$$T_c = T_{lattice} e^{-1/NV}$$

timeline of maximum superconducting transition temperature T_c

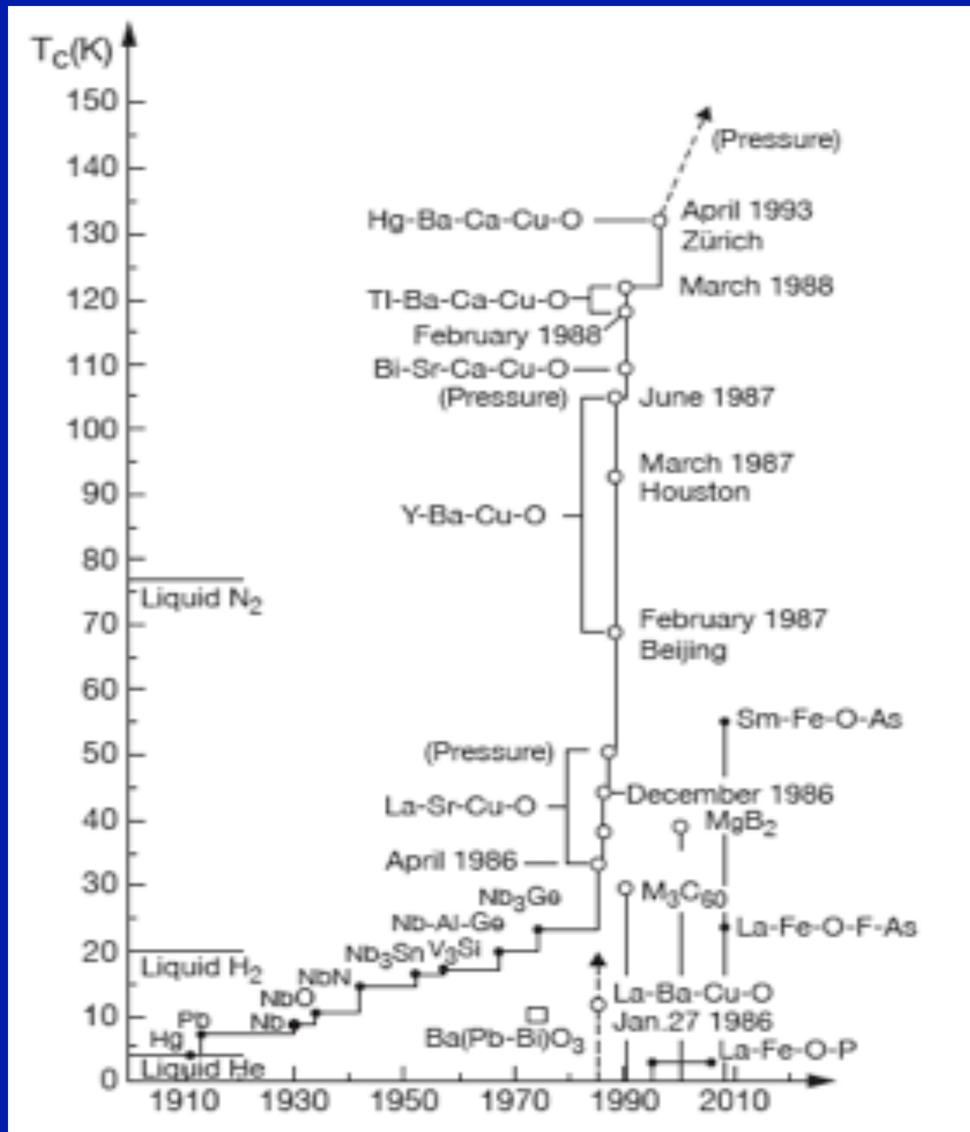

Superconductivity at the border with Magnetism

- superconducting/magnetic interface competition —› co-habitation —› marriage
- vast broadening of materials phase space

of the transition temperature with valene electron concentration. However, the maxima for the magnetic-moment plot coincide with the minima for the transition-temperature plot.

An interesting case is the depression of the transition temperature of Ru by the addition of small amounts of Cr, up to 20 at. % Cr, which also seems to be due to a magnetic interaction. For higher concentrations of Cr the magnetic interaction disappears, as had been observed in the Cr–Ir system, and for Ru solid solutions containing more than 30 at. % Cr the variation in transition temperature with composition is in accord with the empirical rules.

The effect of magnetic rare-earth elements on the superconducting transition temperature of La has been investigated in detail. The lowering of the transition temperature by the rare-earth element seems to be correlated chiefly with the projection of the spin on the orbit of the solute atoms and not with an increase of the effective moment. The effective magnetic moments and spins of the rare-earth elements follow Van Vleck's well-known curve, given in Fig. 2. The superconducting transition temperatures of solid solutions of La containing 1 at. % of rare-earth element are shown in Fig. 3. It was also concluded from these studies that the depression was essentially symmetrical with respect to Gd. The results of additional studies indicate that a deviation from the symmetrical behavior occurs in La–Nd and in La–Er solid solutions. The transition temperature of La is lowered much more rapidly by Nd than by Er. Both elements have the same spin but the effective magnetic moment of Er is much larger than that of Nd. Here again a larger effective moment increases the transition temperature rather than decreasing it. Theoretical calculations which attribute the lowering of the transition temperature by the rare-earth solute to the lowering of the free energy of the normal state by the polarized spins give a reasonable interpretation of the data.

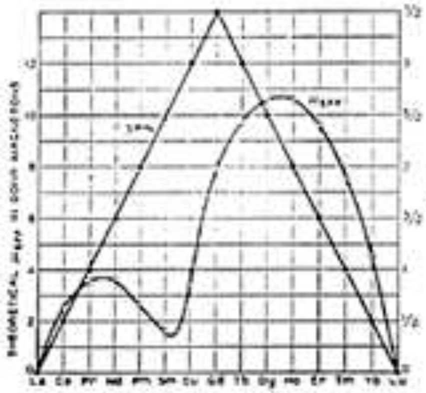

Fig. 2. Effective magnetic moments and spins of the rare earth elements.

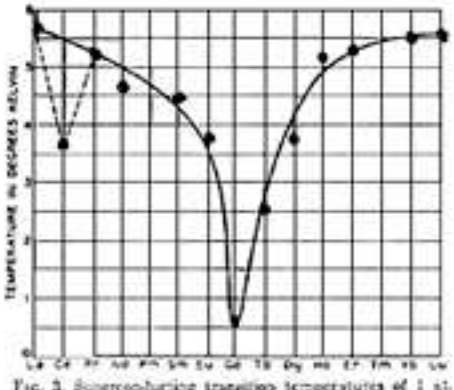

Fig. 3. Superconducting transition temperatures of 1 at. % rare earth solid solutions in La.

Transition–nontransition elements. The superconducting transition temperature is always lowered by the formation of solid solutions between transition and nontransition elements, regardless of how N varies. For example, the transition temperature of Nb is increased by solid-solution formation with any transition element with $N < 5$. The addition of Zr ($N = 4$) raises the transition temperature to about 11°K for a solid solution containing 20 to 30 at. % Zr, whereas the addition of Sn ($N = 4$) lowers the transition temperature to 5.6°K for a solid solution containing 5 at. % Sn.

2. Intermediate Phases

Nontransition elements. The variation of transition temperature with composition has been studied for

B. T. Matthias, H. Suhl, and E. Corenzwit, Phys. Rev. Letters 1, 92 (1958).
B. T. Matthias, H. Suhl, and E. Corenzwit, J. Phys. Chem. Solids 13, 156 (1960).
J. H. Van Vleck, *The Theory of Electric and Magnetic Susceptibilities*, (Oxford University Press, London, 1932), p. 243.
W. Baltensperger, Helv. Phys. Acta 32, 197 (1959).
H. Suhl and B. T. Matthias, Phys. Rev. Letters 2, 5 (1959).
A. Maradudin and J. Peretti, Compt. Rend. 248, 2850 (1959).

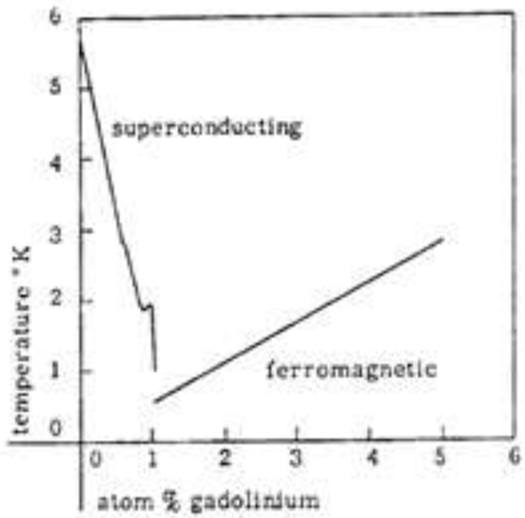

Figure 8-1

Superconducting and ferromagnetic transition temperatures of La Gd alloys [after B. T. Matthias, *IBM J.*, 6, 250(1962)]. Note the sharp drop of the superconducting transition point when the (magnetic) gadolinium atoms are added to lanthanum.

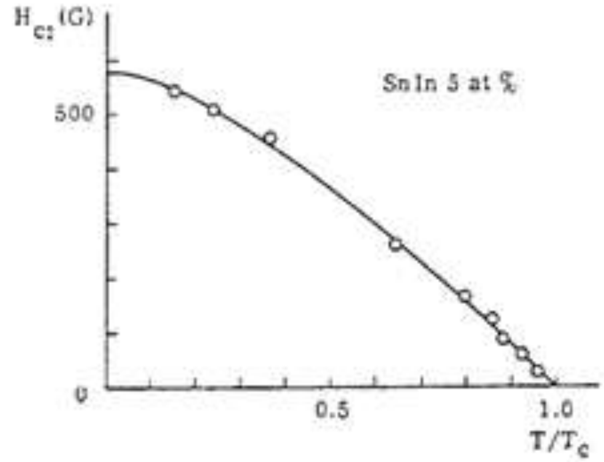

Figure 8-2

Relation between temperature and field at the upper transition point of a "dirty" Type II superconductor. Experimental points by E. Guyon and A. Martinet. The theoretical curve is derived from Eq. (8-40).

High-Temperature Superconductors, the First Ternary System

Abstract. *A new system of high-temperature superconductors is reported. The compounds, $Mo_{6-x}A_xS_6$ where A is Cu, Zn, Mg, Ag, Cd, Sn, or Pb, are rhombohedral with* a $\simeq$ *6.5 angstroms and* $\alpha \sim 90°$*. The transition temperatures range from* $\sim 2.5°K$ *for the Cd compound to* $\sim 13°K$ *for the Pb compound.*

During the last few years a number of new superconductors have been discovered among the transition metal chalcogenides. Most of these are layer compounds in which the sequence of layers is -S-S-M-S-S-M-, where M is a transition metal. The metal-to-metal interactions between layers are weak and the compounds have a pseudo two-dimensional network of metal atoms. It is possible to intercalate these compounds with, for example, alkali metals, and in this case the highest reported superconducting transition temperature is $\sim 4.5°K$ for K_xMoS_2 (*1*). However, where a structure containing a true three-dimensional network of metal atoms is synthesized from similar elements, the transition temperatures are much higher, for example, $\sim 13°K$ for $Li_{0.8}Ti_{1.1}S_2$ (*2*).

In our search for new chalcogenides with a three-dimensional network of metal atoms, we found an entirely new system of high-temperature superconductors: $Mo_{6-x}A_xS_6$, where A is Cu, Mg, Zn, Cd, Ag, Sn, or Pb. These compounds were first synthesized by Chevrel *et al.* who mixed the elements or the sulfides in quartz ampoules at

Table 1. Superconductivity of ternary molybdenum sulfides.

Composition	Superconducting transition temperature (°K)	Lattice constants * (A)			
		Rhombohedral axes		Hexagonal axes	
		a	α	*a*	*c*
$Mo_{4.8}Cu_{1.8}S_6$	10.9–10.8	6.51	95°18′	9.63	10.18
Mo_5ZnS_6	3.0– 2.7	6.489	94°41′	9.545	10.282
$Mo_{4.8}Ag_{1.2}S_6$	8.9– 8.4	6.48	91°57′	9.32	10.83

Proc. Natl. Acad. Sci. USA
Vol. 74, No. 4, pp. 1334–1335, April 1977
Physics

High superconducting transition temperatures of new rare earth ternary borides

(ferromagnetism/superconductors)

BERND T. MATTHIAS*, E. CORENZWIT, J. M. VANDENBERG, AND H. E. BARZ

Bell Laboratories, Murray Hill, New Jersey 07974

Contributed by Bernd T. Matthias, January 14, 1977

ABSTRACT A new group of ternary borides has been found that show either ferromagnetism or superconductivity. Their general formula is MRh_4B_4 where M is a transition or rare-earth element. Their superconducting transition temperatures range from approximately 2.5 K for the Sm compound to approximately 12 K for the Lu compound.

In the past, the superconducting transition temperatures of borides have always been rather low. The highest values in the

Table 1. Superconducting transition temperatures

Compound*	T_c range, K
YRh_4B_4	11.34–11.26
$NdRh_4B_4$	5.36–5.26
$SmRh_4B_4$	2.51–2.45
$ErRh_4B_4$	8.55–8.49

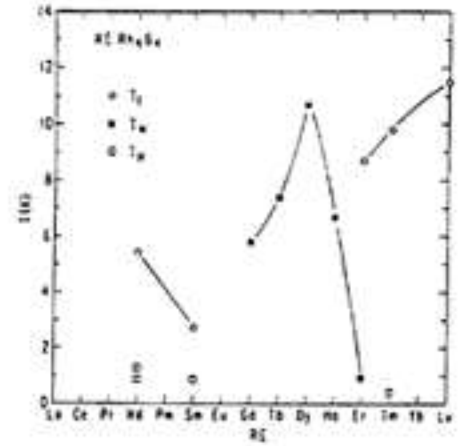

Fig.1.11. Superconducting critical (T
Néel (T_N) and Curie (T_M) temperatures
$RERh_4B_4$ compounds. From [Ref.1.18, Ch

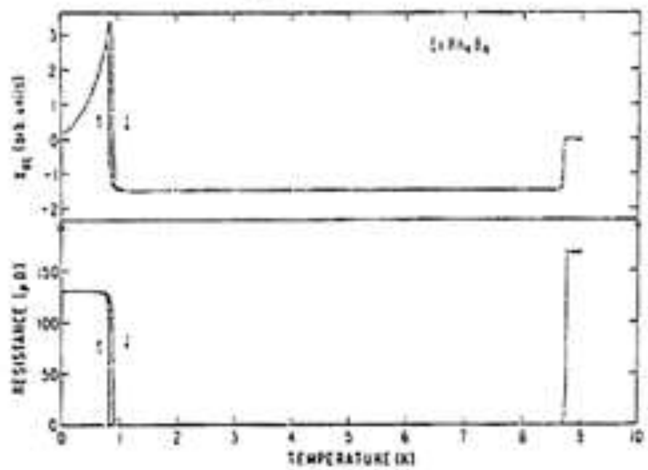

Fig.1.12. Typical ac
tic susceptibility χ_{ac}
electrical resistance-
temperature data for E
[1.75]

compounds has been the interplay between superconductivity and long-range magr
order [Ref.1.18, esp. Chap.4]. Like the $REMo_6X_8$ compounds, the $RERh_4B_4$ compour
have an ordered RE sublattice and superconducting and magnetic states with cor
able free energies. This latter aspect is apparent in Fig.1.11 in which the su
conducting and magnetic critical temperatures of the $RERh_4B_4$ compounds are plc
versus RE. All of the superconducting $RERh_4B_4$ compounds in which the RE 4f ele
shell is partially filled undergo some type of magnetic ordering below T_c, at
peratures T_M in the vicinity of 1 K. Whereas $ErRh_4B_4$ becomes ferromagnetic [1.
$NdRh_4B_4$ [1.70,71], $SmRh_4B_4$ [1.72], and $TmRh_4B_4$ [1.73,74] exhibit antiferromagr

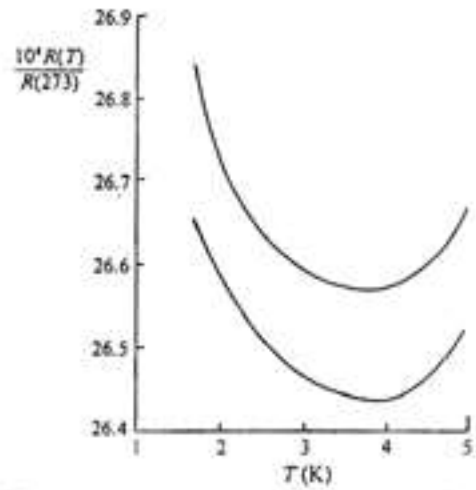

Figure 1 The minimum in the electrical resistivity of *Au* (de Haas, de Boer and van den Berg, 1934).

3d transition metal impurities such as *Fe*, dependent on the impurity concentration.

The resistance minimum as observed in *Au* is shown in figure 1, reproduced from the 1953 edition of *The Theory of Metals* by A.H. Wilson, one of the standard texts of this period. The reason for the minimum was not known at that time and Wilson comments, 'the cause of the minimum is entirely obscure and constitutes a most striking departure from Mathiessens's rule, according to which the ideal and residual resistances are additive — some new physical principle seems to be involved'. A very significant advance in the theory of magnetic impurities was an explanation of this effect by J. Kondo in 1964.

Early theoretical work on impurities in metals in the late 50s by J. Friedel and associates concentrated on explaining the trends in the behaviour as the impurity elements are varied across the transition element series. The most important concept to emerge from this work was that of 'virtual bound states' ; states which are almost localized due to resonant scattering at the impurity site. A different formulation of this idea was put forward by P.W. Anderson (1963), in a version now known as the 'Anderson model': this model has played a very important role in

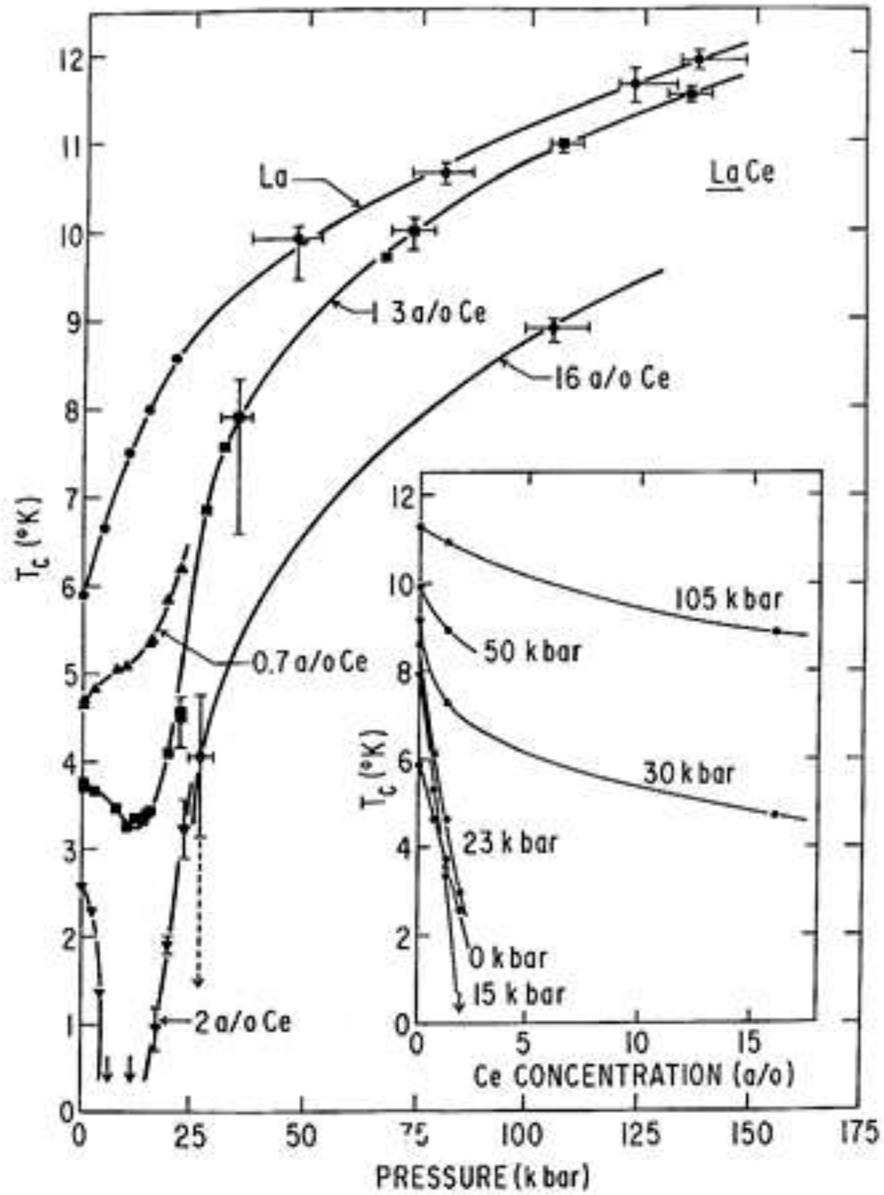

M. B. Maple, J. Wittig, and K. S. Kim, *Phys. Rev. Lett.* 23, 1375 (1969)

1979: Heavy Fermions: superconductivity marries magnetism, its enemy, in $CeCu_2Si_2$ ($T_c = 0.5K$)

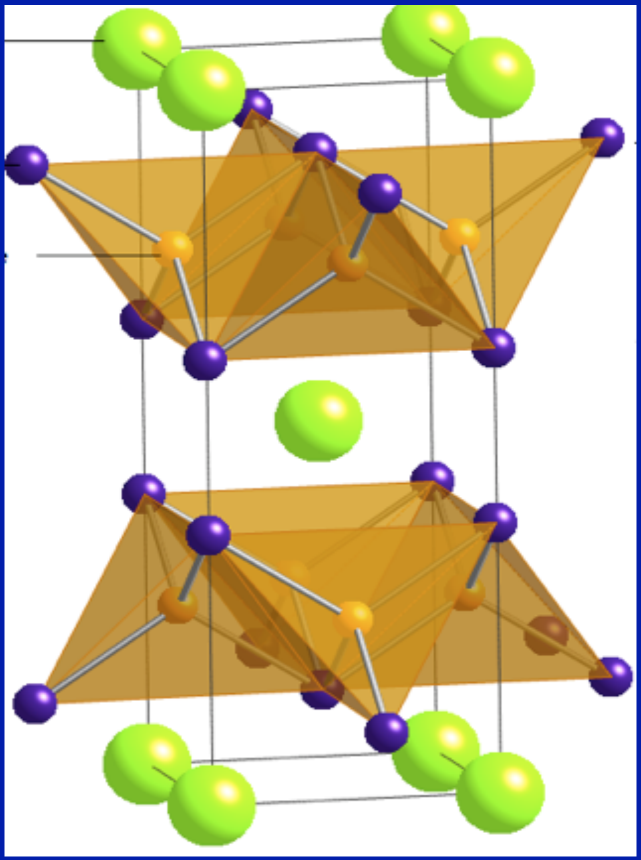

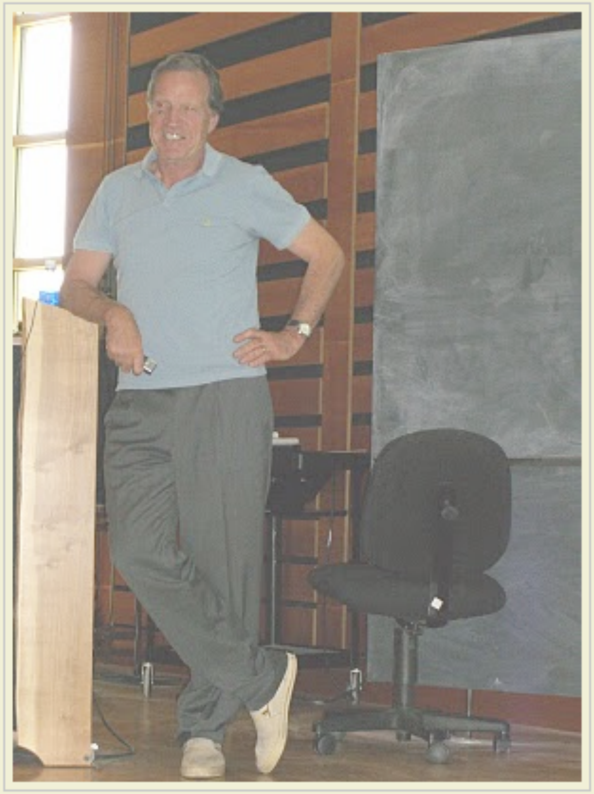

Frank Steglich (MPI CPfS, Dresden) Pictures to be added.

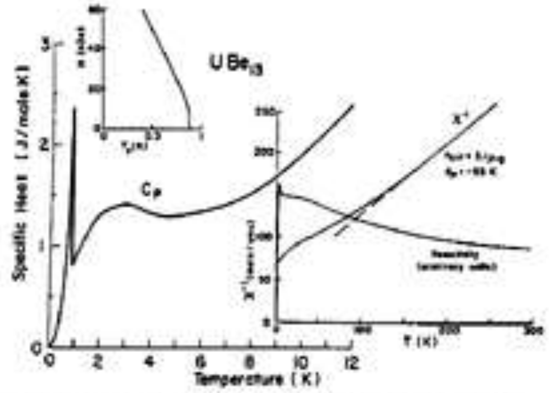

Fig. 1. Temperature dependence of selected properties of UBe_{13}.

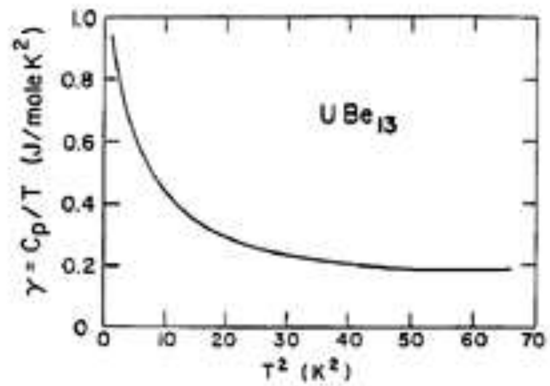

Fig. 2. Low temperature specific heat of UBe_{13}.

* Permanent address: Laboratorium für Festkörperphysik, ETH-Hönggerberg, CH-8093 Zürich, Switzerland.

0304-8853/85/$03.30 © Elsevier Science Publishers B.V. (North-Holland Physics Publishing Division)

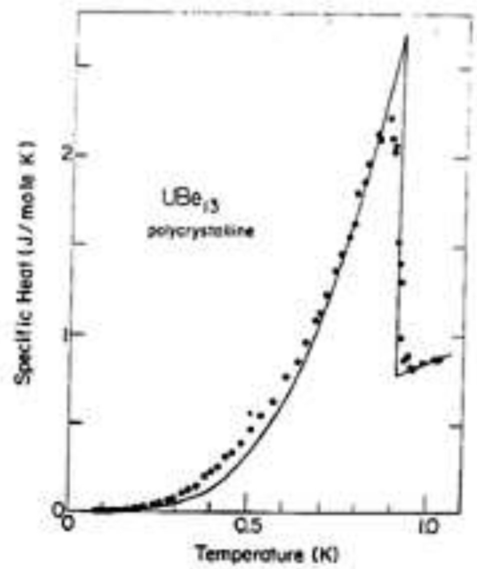

Fig. 3. Comparison of superconducting specific heat anomaly in UBe_{13} with strong coupling ABM p-wave calculation [10].

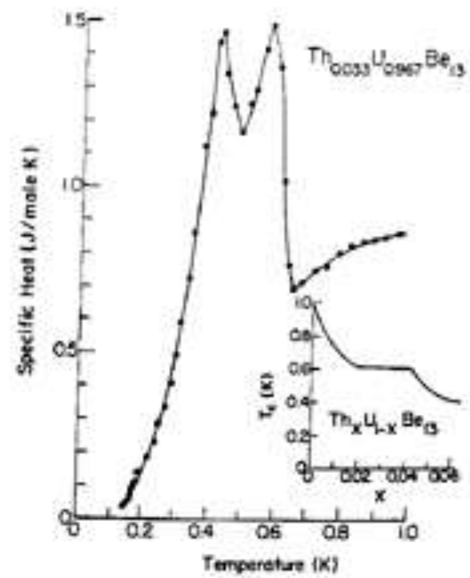

Fig. 4. Low temperature specific heat of a $U_{0.967}Th_{0.033}$ polycrystal, inset schematically shows depression of T_c wi addition to UBe_{13}.

Mathur et al. Nature **394**, 39 (1998)

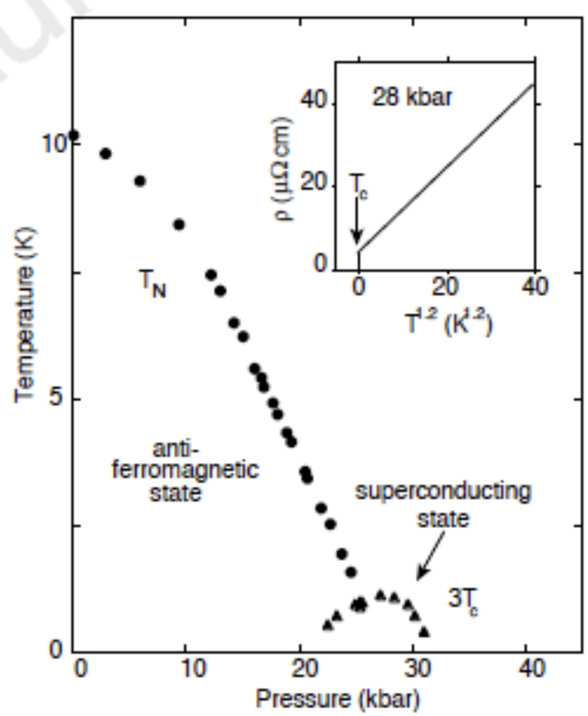

Figure 2 Temperature–pressure phase diagram of high-purity single-crystal $CePd_2Si_2$. Superconductivity appears below T_c in a narrow window where the Néel temperature T_N tends to absolute zero. Inset: the normal state *a*-axis resistivity above the superconducting transition varies as $T^{1.2\pm0.1}$ over nearly two decades in temperature[27,30]. The upper critical field B_{c2} at the maximum value of T_c varies near T_c at a rate of approximately −6 T/K. For clarity, the values of T_c have been scaled by a factor of three, and the origin of the inset has been set at 5 K below absolute zero.

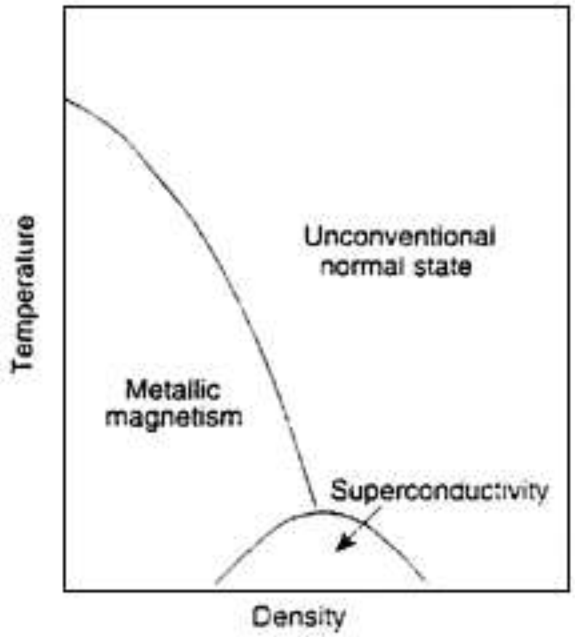

Figure 1 Possible temperature–density phase diagram of a pure metal in which magnetic order is quenched gradually with increasing lattice density. Near the critical density n_c, where the magnetic transition temperature vanishes, magnetic interactions become strong and long-range. The normal state is expected to be anomalous here and, at sufficiently low temperatures, it is expected to give way to a kind of superconductivity in which Cooper pairs are bound together by a glue of magnetic origin. Superconductivity may exist only over a very narrow range of densities near n_c–which is where magnetic interactions overwhelm other channels. Moreover, superconductivity may exist only in samples in which the carrier mean free path exceeds the superconducting coherence length. In most cases this requires samples of very high purity.

Phase diagram of $CeRhIn_5$ (Park and Thompson)

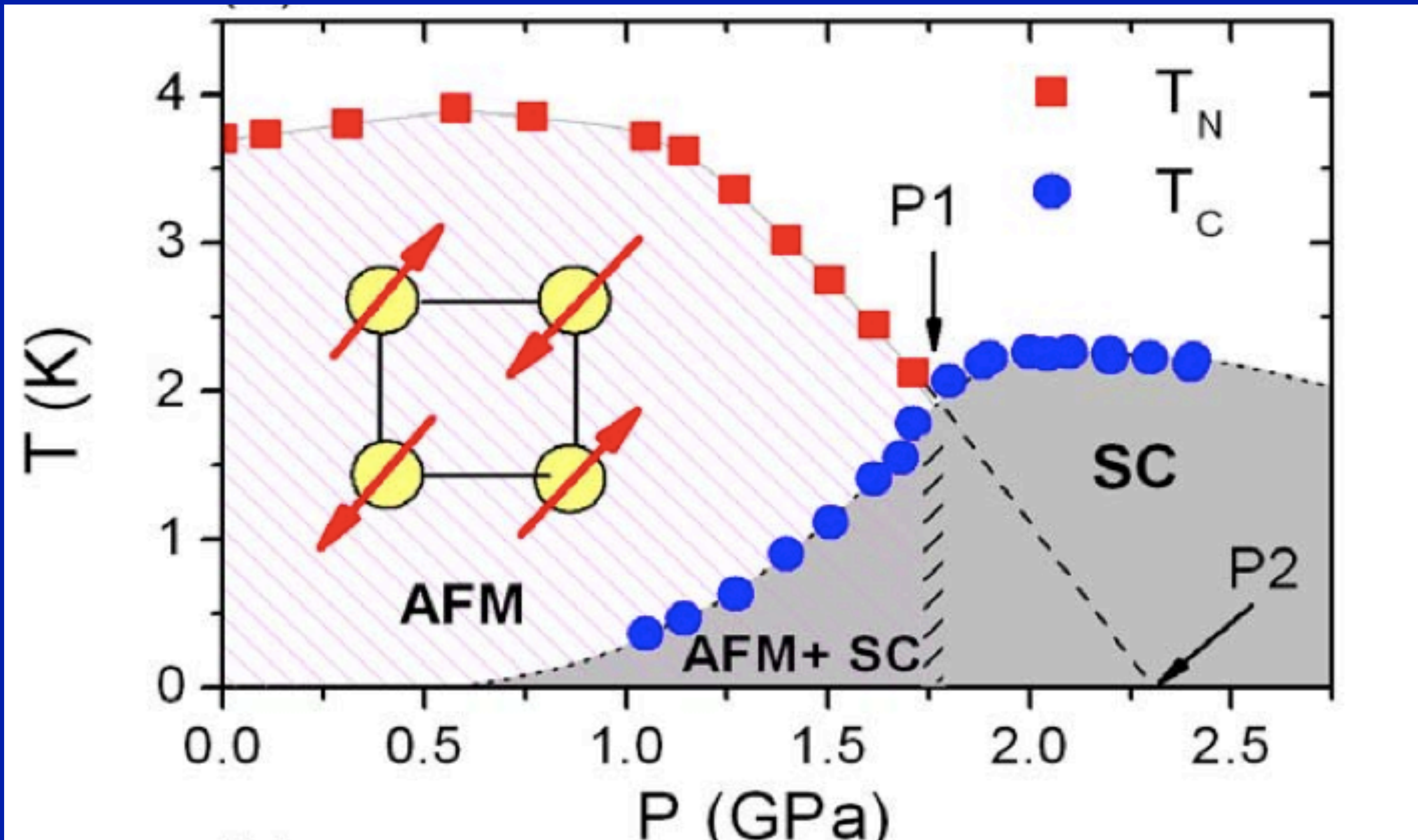

What happens at T_c in heavy Fermions?

- Superconductivity opens a gap in the electronic spectrum at the Fermi surface
- The electronic spectrum carries strong magnetic fluctuations that can mediate superconductivity or magnetic order
- Establishing superconductivity can be seen as resolving the opposed conflict of local moment magnetism versus non-local itinerant electronic states

Stock et al.   Phys. Rev. Lett. **100**, 087001 (2008)

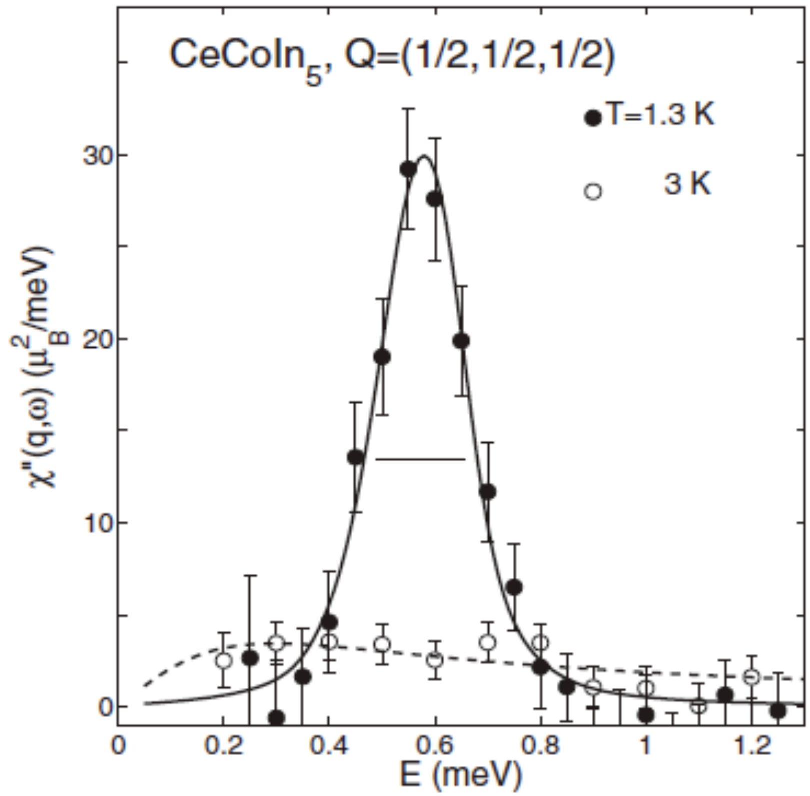

FIG. 1. The imaginary part of the dynamic susceptibility at $\mathbf{Q} = (\frac{1}{2}\,\frac{1}{2}\,\frac{1}{2})$ is plotted in the normal (3 K) and in the superconducting (1.35 K) states. A background taken at $\mathbf{Q} = (0.3, 0.3, 0.5)$ and $\mathbf{Q} = (0.7, 0.7, 0.5)$ was subtracted. The horizontal bar is the resolution width.

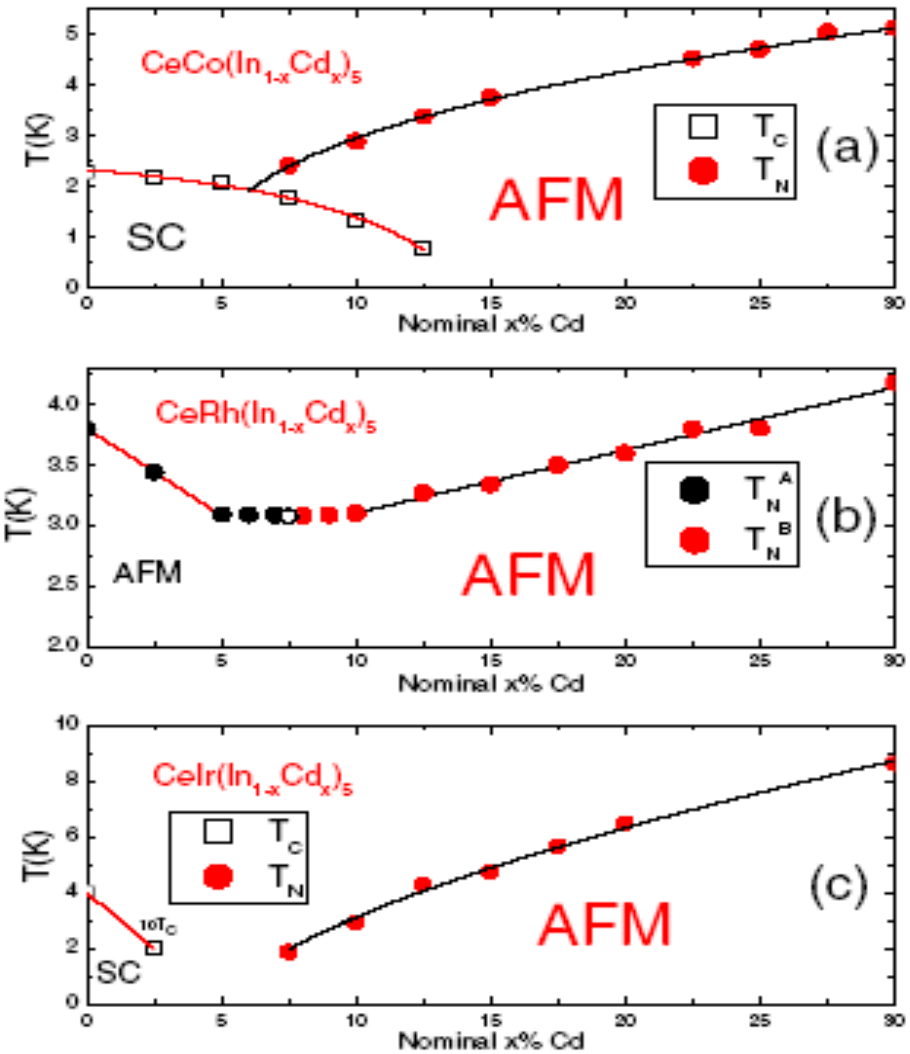

FIG. 2 (color online). Dependence of superconducting transition temperatures T_c and Néel temperatures T_N on x, where x is the nominal Cd content of crystals. See text for details. (a) $CeCo(In_{1-x}Cd_x)_5$, (b) $CeRh(In_{1-x}Cd_x)_5$, and (c) $CeIr(In_{1-x}Cd_x)_5$. For (b), $T_N{}^A$ and $T_N{}^B$ are associated with different antiferromagnetic (AFM) phases as discussed in the text. T_c and T_N were extracted from specific heat (Fig. 1) and confirmed with magnetic susceptibility measurements.

M. Nicholas et al. Phys. Rev. B **76**, 052401 (2007)

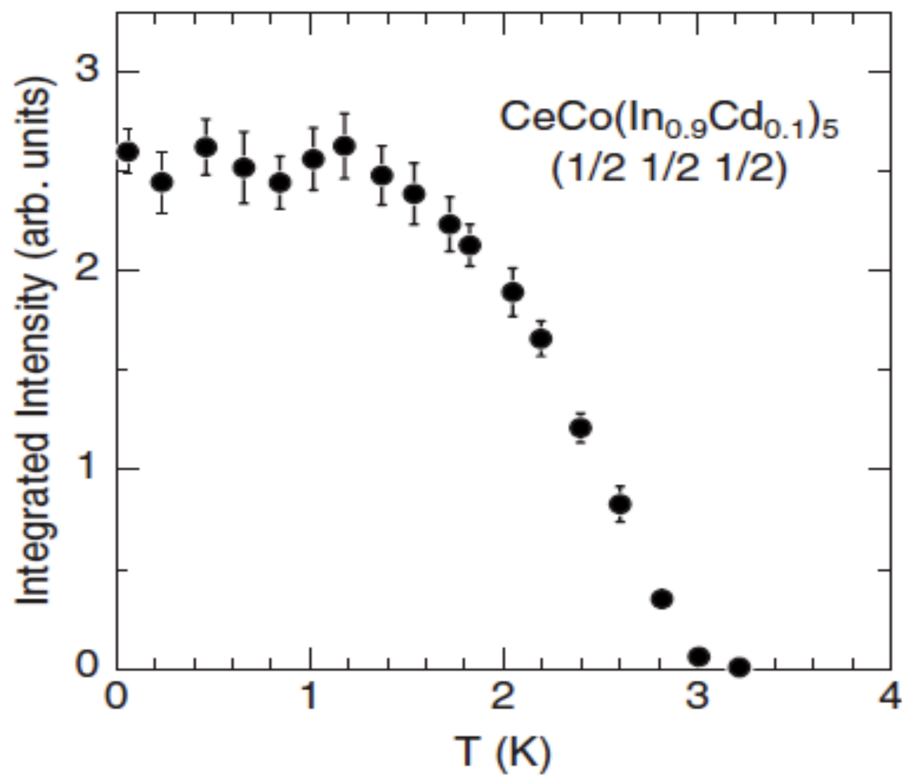

FIG. 4. Temperature dependence of the integrated magnetic intensity as obtained by Gaussian fits to the scans across $Q = (\frac{1}{2}, \frac{1}{2}, \frac{1}{2})$.

1986: the new age of cuprates

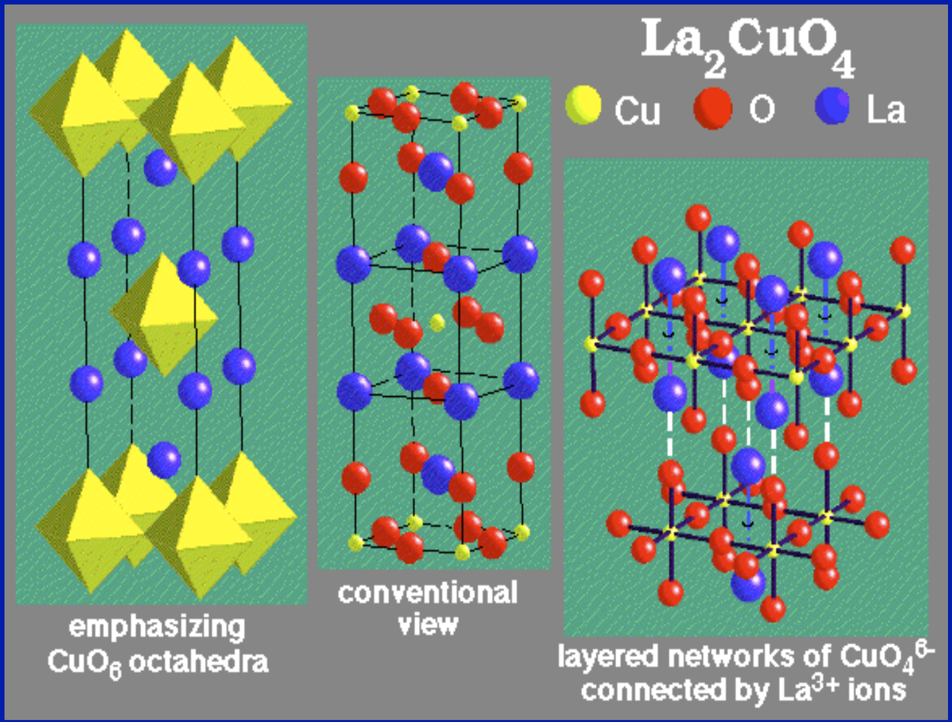

Alex Müller in 2001.

$La_{1.84}Sr_{0.16}CuO_4$ T_c = 40K

generic cuprate phase diagram

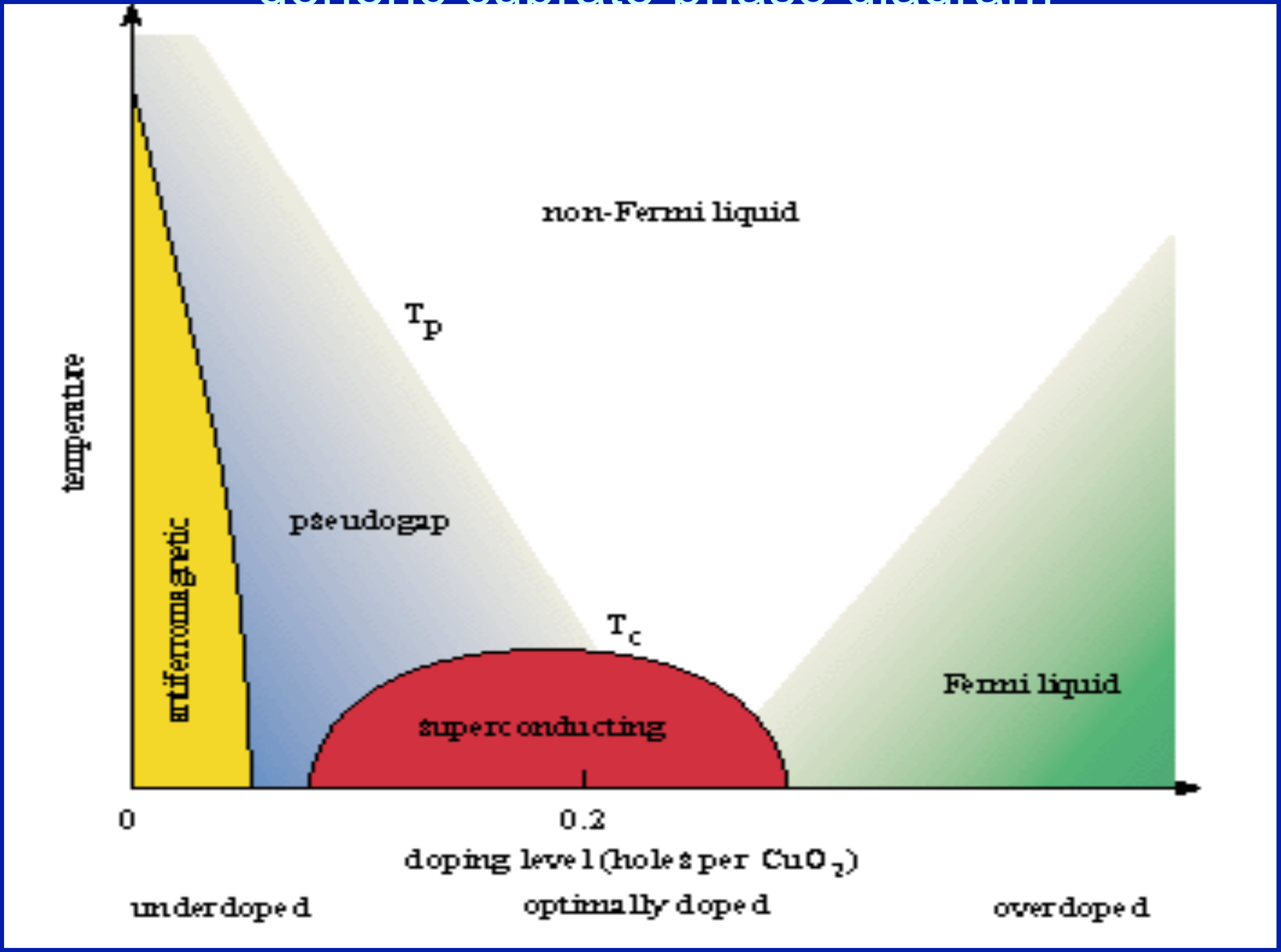

the new iron age: pnictides T_c = 56K

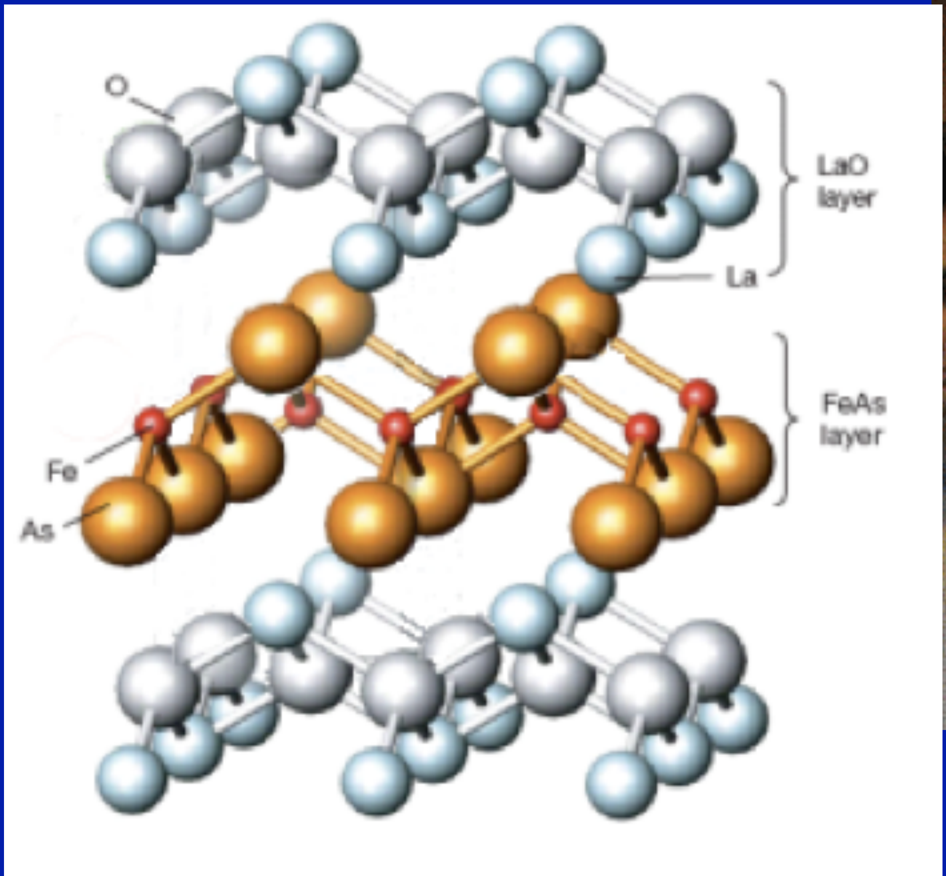

Wolfgang Jeitschko

the path to this new material

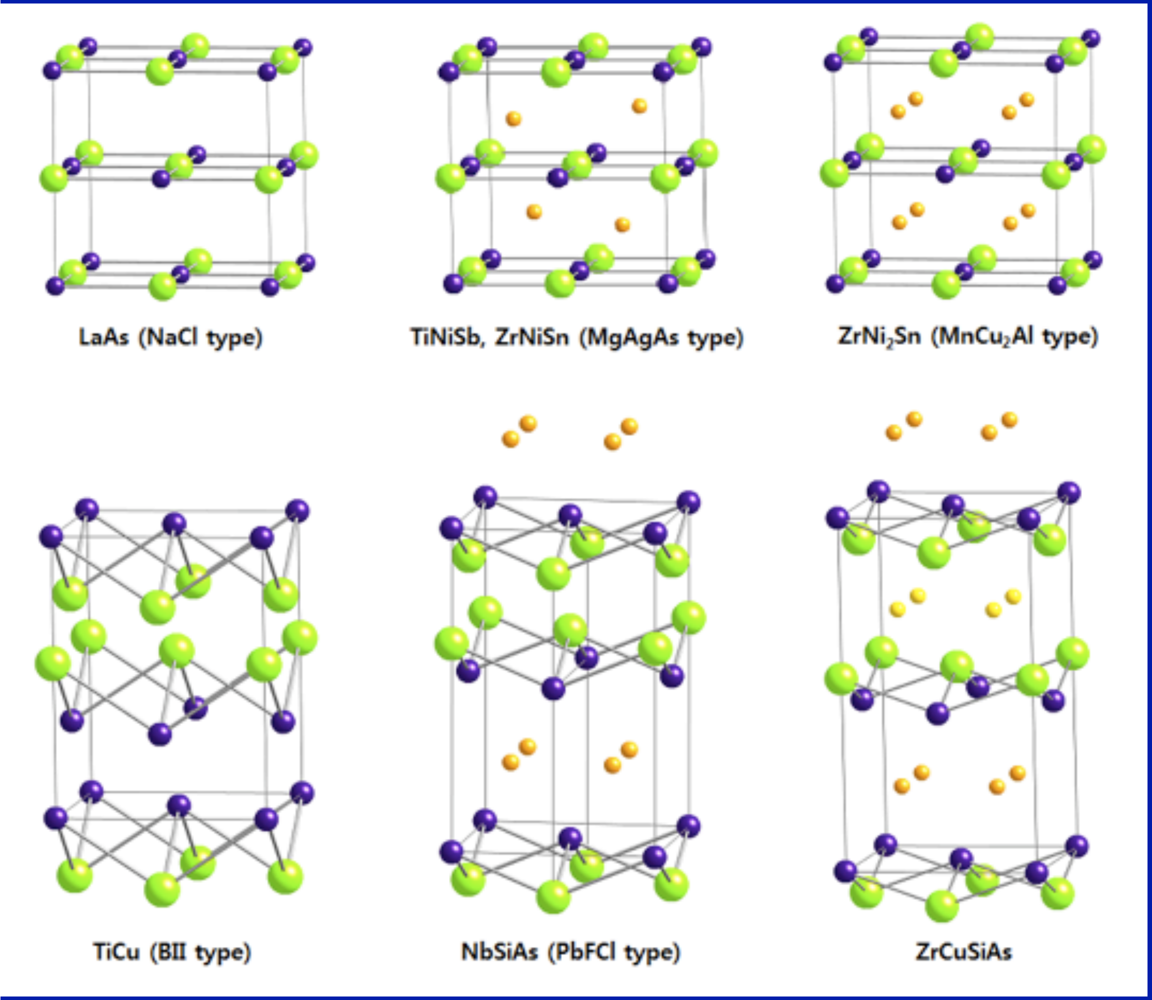

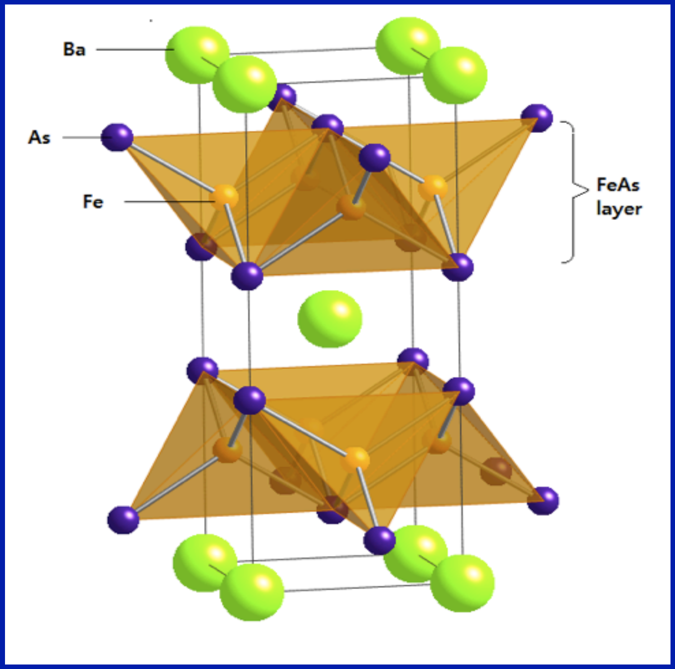

ELSEVIER

Journal of Alloys and Compounds 229 (1995) 238–242

Journal of ALLOYS AND COMPOUNDS

The rare earth transition metal phosphide oxides LnFePO, LnRuPO and LnCoPO with ZrCuSiAs type structure

Barbara I. Zimmer, Wolfgang Jeitschko, Jörg H. Albering, Robert Glaum, Manfred Reehuis

Anorganisch-Chemisches Institut, Universität Münster, Wilhelm-Klemm-Strasse 8, D-48149 Münster, Germany

Received 3 April 1995

Abstract

The compounds LnFePO (Ln = La–Nd, Sm, Gd), LnRuPO (Ln = La–Nd, Sm, Gd) and LnCoPO (Ln = La–Nd, Sm) crystallize with the tetragonal ZrCuSiAs type structure ($P4/nmm$, $Z = 2$), which was refined from single-crystal X-ray data of PrFePO ($a = 391.13(6)$ pm, $c = 834.5(2)$ pm, $R = 0.026$) and CeRuPO ($a = 402.6(1)$ pm, $c = 825.6(2)$ pm, R = 0.018). The refinement of the occupancy parameters showed the oxygen position to be fully occupied in both compounds. The oxygen content of the samples was also proven by EDAX analyses. The structures of the compounds SmFePO and LaCoPO were refined by Rietveld analyses of X-ray powder data.

Keywords: Rare earth metals; Transition metal phosphide oxides; Crystal structure

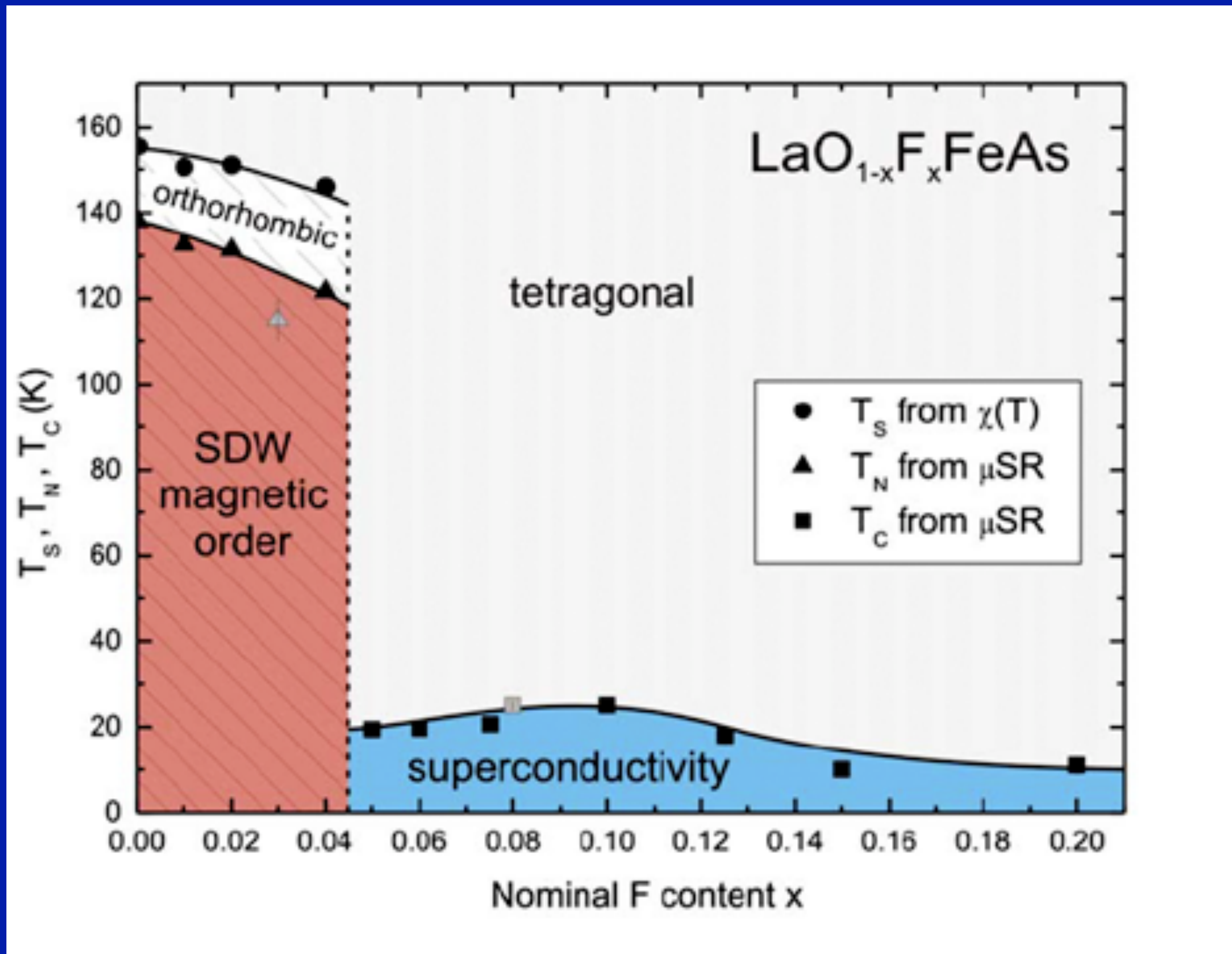

M. Norman Physics 1 (2008) 21

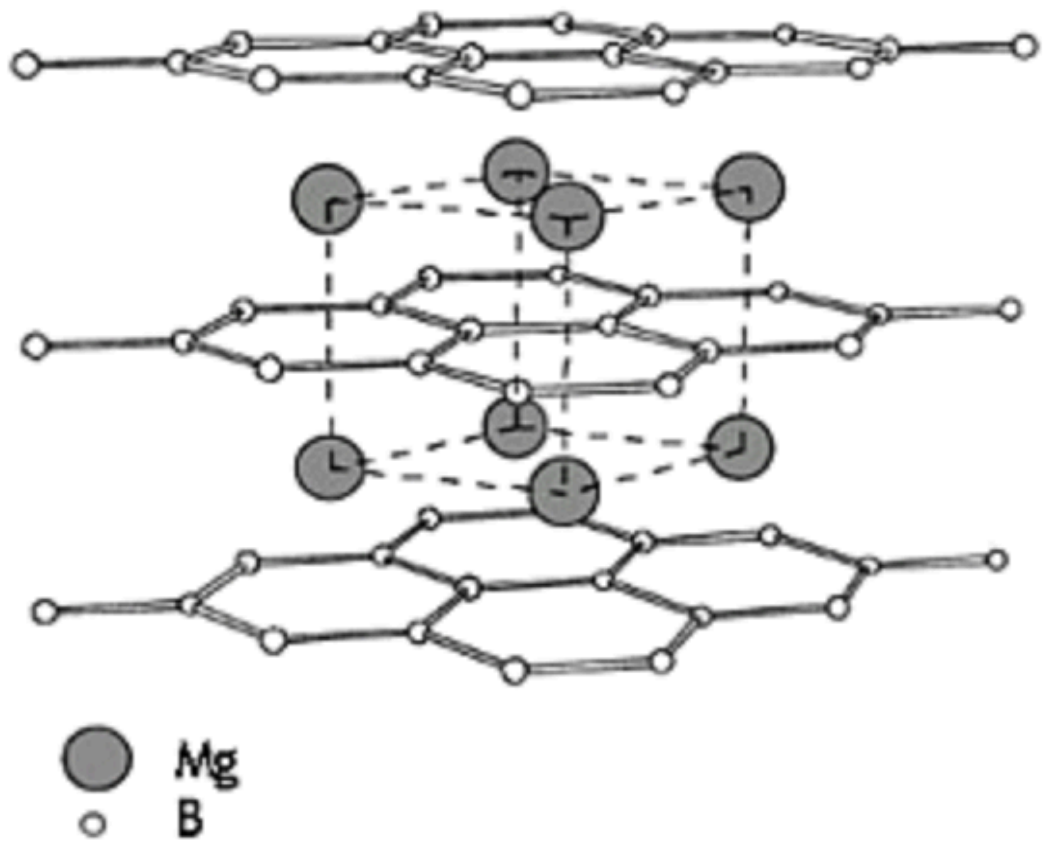

Schematic of the crystal structure of MgB_2.

letters to nature

Superconductivity at 25.5 K in electron-doped layered hafnium nitride

Shoji Yamanaka*†, Ken-ichi Hotehama* & Hitoshi Kawaji*

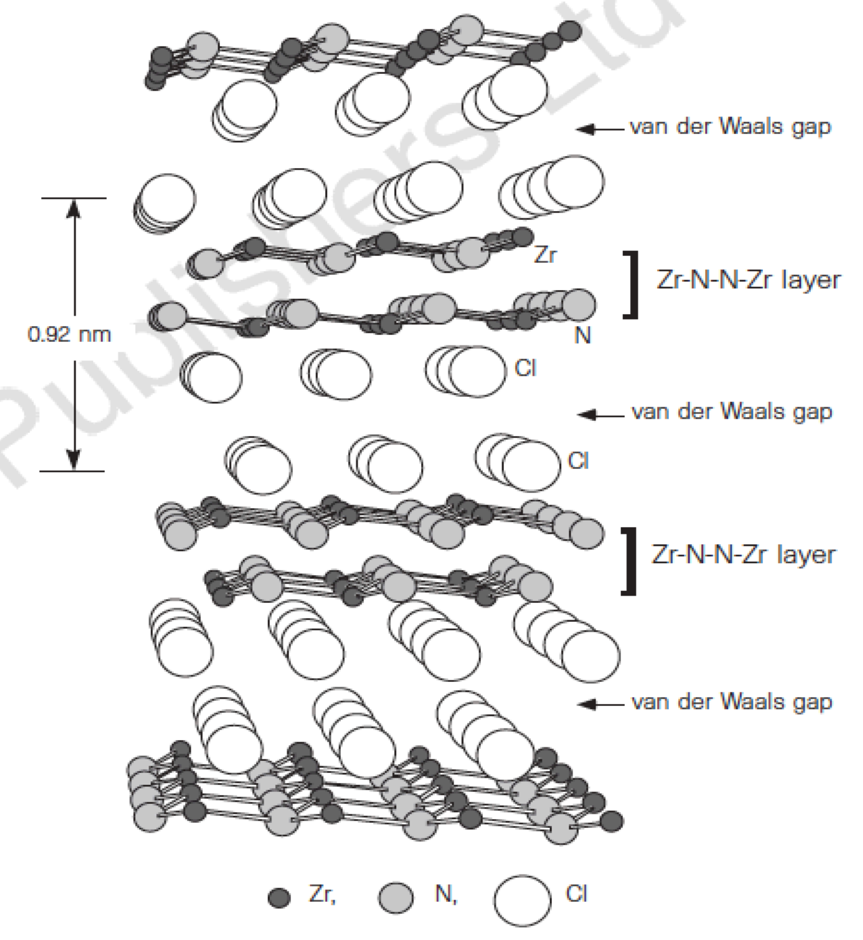

Figure 1 Structural model of β-ZrNCl (ref. 5) (isostructural with β-HfNCl).

Onward and upward?

- the record says that T_c is raised by finding new classes of materials
- maximum T_c within each class appears near a boundary separating local and non-local physics
- no obvious maximum to T_c